Supporting Information

Andreev et al. 10.1073/pnas.0914330107

SI Text

OCD Measurements. For oriented circular dichroism measurements we prepared the supported bilayer on quartz slides with spacers of 0.2 mm thickness on one side with special polish for far UV measurements (Starna). The procedure of slides cleaning included the following steps: 1) soaking in cuvette cleaner solution for 5–10 min, 2) rinsing with de-ionized distilled water, 3) sonicating for 10 min in 2-propanol, 4) sonicating in acetone, 5) sonicating in 2-propanol once again, 6) rinsing with de-ionized water, 7) soaking for 30 min, first, in 30% hydrogen peroxide, 8) and later in 70% sulfuric acid, and 9) rinsing with Milli-Q purified water. A POPC lipid monolayer was deposited on a quartz substrate by the Langmuir-Blodgett (LB) method using (KSV minitrough). For the LB deposition, a clean wet slide was immersed vertically into the clean subphase (Milli-Q purified water kept at 25 °C) of a Langmuir-Blodgett trough. Then small amount of POPC lipid in chloroform was spread on the surface of the subphase and allowed solvent to evaporate for about 20 min. Next, the monolayer was compressed to 32 mN/m. When the surface pressure was stabilized the slide was pulled out form the subphase with speed of 10 mm/min. The second layer was created by fusion with POPC vesicles. About 60 μl of LUV vesicles (100 nm in diameter, lipid concentration of 2 mM) was spread on the slides for 30 min, then slides were rinsed carefully and filled with pH 4 phosphate buffer (80 μl of buffer for each slide). The slides were stacked together while filling with the buffer to have a complete set of 12 slides (24 bilayers). The spacers between slides kept them form the sticking to each other. The quality of the supported bilayers were accessed in separate experiment by using fluorescent vesicles for fusion, and analyzing roughness of the obtained supported bilayer under the fluorescent microscope (Olympus IX71). Once the blank OCD spectrum was measured the slides were carefully disassembled and filled with phosphate buffer pH4 containing 10 μM pHLIP peptide and the OCD spectrum of the sample was recorded. The blank spectrum was subtracted from the sample spectrum to get final line presented in Fig. 1*D*.

Additional details of the stopped-flow fluorescence and CD measurements The concentration of the peptide (7 μM), lipids (1 mM) before mixing and mixing conditions (6.5 mL/sec flow of each solution) were optimized to ensure: *i*) the proper rapid mixing of the entire volume of the sample to get the target changes of pH (from pH8 to pH4 and vice versa); *ii*) the best signal to noise ratio, and *iii*) minimal disruption of liposomes, which was assessed by changes of the scattered light signal. At the peptide: lipid ratio of 1:142 we used in these experiments, the equilibrium binding strongly favors the membrane-bound state II [by 6–7 kcal/mol according to our previously published thermodynamic studies (1)]. Changes of the pHLIP fluorescence signal were recorded through a 320 nm cutoff filter using an excitation wavelength of 280 nm. The fluorescence signal was corrected for photobleaching. Changes of the scattered light signal from the liposomes were recorded through the 320 nm cutoff filter using an incident light with wavelength of 320 nm. Each kinetic curve was recorded several times and then averaged, excluding the first 3–4 shots. The shift of the entire fluorescence spectrum during folding/unfolding was also recorded in a global mode using an emission monochromator, with an excitation wavelength of 275 nm to minimize scattered light at short wavelengths (in a separate experiment the spectra were recorded with 280 nm of the excitation wavelengths). Each spectrum was recorded several times and averaged. All spectra were corrected for the spectral sensitivity of the instrument by comparing the spectrum of a tryptophan solution obtained with the same instrument with a standard tryptophan spectrum. In a control experiment, the signal was measured from the liposomes in the absence of peptide. At an excitation of 275 nm the scattering signal was insignificant, even at short wavelengths of the spectra.

The most challenging measurement was to monitor the changes of the CD signal (at 225 nm), about 90% of which occurred within the first second, approximately 100 times faster than the fluorescence changes. About 20 shots were performed and signals were averaged. The sensitivity might be enhanced by increasing the peptide concentration. However, there are two serious obstacles to such an approach: i) at high peptide concentration the equilibrium in solution is shifted toward aggregated forms, which might differently interact with the lipid bilayer; ii) any increase of the peptide concentration must be accompanied with an increase of lipid concentration to fully favor the bound state and minimize amount of the unbound peptide, but high liposome concentrations result in the appearance of significant light scattering, which interferes with the CD signal. To reduce light scattering, small POPC vesicles (approximately 50 nm in a diameter) were used in the study for both CD and fluorescence kinetic runs. In a separate experiment we confirmed that there is no significant difference between the kinetics curves of pHLIP interacting with vesicles of 50 and 100 nm in diameter. In order to accurately establish the baseline in CD kinetics experiments, we recorded the signal alteration in response to the pH changes in a mode without triggering; in this mode the rapid changes could not be monitored and this mode was used only for the detection of the initial and final states of the process. Thus, the CD signal changes varied from -5 to $-14 \div -15$ millidegree and vice versa.

The baseline and asymptotic values are extremely important for accurate fitting of the experimental data. Stopped-flow fluorescence measurements of the peptide insertion into the lipid bilayer were performed at various temperatures. All solutions were pre-equilibrated at each experimental temperature before the measurements. To ensure that the process of peptide insertion and exist is completed for all temperatures, we investigated fluorescence changes at the same temperatures in state mode. In a range of investigated temperatures the absolute increase of fluorescence signal was the same (about 55–60% of increase).

Kinetic Model. The rate equations for the time dependence can be written as differential equations:

$$-\frac{d[I_1]}{dt} = k_1[I_1] - \frac{d[I_2]}{dt} = k_2[I_2] - k_1[I_1] - \frac{d[I_3]}{dt} = k_3[I_3] - k_2[I_2] - \frac{d[I_4]}{dt} = k_4[I_4] - k_3[I_3] - \frac{d[I_5]}{dt} = k_4[I_4] \quad \text{[S1]}$$

These differential equations can be solved analytically and the rate equations integrated, assuming that the initial concentrations of every intermediate except I_1 are zero. The function used for fitting of the experimental data can be written in general form as

$$g(t) = \sum_{i=1}^{n+2} f_i[I_i], \qquad \text{[S2]}$$

where f_i are the changes of fluorescence or CD signals associated with the ith transition from one intermediate to another, and n is the number of intermediates used in the model. For the kinetic model with three intermediates the function used to fit the experimental data is

$$\begin{aligned} g(t) &- f_1 e^{-k_1 t}\frac{k_1(e^{(k_1-k_2)t}-1)}{k_1-k_2} \\ &+ f_3 e^{-k_1 t}\frac{k_1k_2(e^{(k_1-k_3)t}(k_1-k_2)+e^{(k_1-k_2)t}(k_3-k_1)+(k_2-k_3))}{(k_1-k_2)(k_1-k_3)(k_2-k_3)} \\ &+ f_4 e^{-k_1 t}\frac{k_1k_2k_3}{(k_2-k_1)(k_2-k_3)(k_3-k_1)(k_2-k_4)(k_3-k_4)(k_4-k_1)} \\ &\times \begin{pmatrix} e^{(k_1-k_3)t}(k_1-k_2)(k_1-k_4)(k_2-k_4) \\ -e^{(k_1-k_4)t}(k_1-k_2)(k_1-k_3)(k_2-k_3)- \\ e^{(k_1-k_2)t}(k_1-k_3)(k_1-k_4)(k_3-k_4) \\ +(k_2-k_3)(k_2-k_4)(k_3-k_4) \end{pmatrix} \\ &+ f_5 e^{-k_1 t}\frac{1}{(k_2-k_1)(k_2-k_3)(k_3-k_1)(k_2-k_4)(k_3-k_4)(k_4-k_1)} \\ &\times \begin{pmatrix} e^{(k_1-k_4)t}k_1k_2k_3(k_1-k_2)(k_1-k_3)(k_2-k_3)- \\ e^{k_1 t}(k_1-k_2)(k_1-k_3)(k_2-k_3)(k_1-k_4)(k_2-k_4)(k_3-k_4)- \\ e^{(k_1-k_3)t}k_1k_2k_4(k_1-k_2)(k_1-k_4)(k_2-k_4)+ \\ e^{(k_1-k_2)t}k_1k_3k_4(k_1-k_3)(k_1-k_4)(k_3-k_4) \\ -k_2k_3k_4(k_2-k_3)(k_2-k_4)(k_3-k_4) \end{pmatrix} \end{aligned} \qquad \text{[S3]}$$

All fluorescence kinetic data were normalized to the initial values, so that f_1 was about 1. The initial value could not be measured exactly due to the dead time of the instrument, which results in monitoring of the kinetic process with some delay. We always perform control shots by mixing pHLIP-POPC with the buffer of the same pH to estimate the initial value, however some uncertainty still exists. Therefore, we gave very limited variability to the initial value during the fitting procedure. From the steady-state experiments performed at various temperatures we established that the absolute increase of fluorescence signal induced by the drop of pH was the same at all temperatures (55–60%). Therefore, asymptotic values (f_5) were chosen to be the same for kinetics runs performed at different temperatures, and the values varied from 1.55 to 1.6.

CD folding and unfolding curves (Fig. 2*A*, *D*) were fitted well using a simpler kinetic model with no intermediates and single intermediate state:

$$g(t) = f_1[I_1] + f_2[I_2]g(t) = f_1[I_1] + f_2[I_2] + f_3[I_3]. \qquad \text{[S4]}$$

For each step, the characteristic times t_i ($t_i = 1/k_i$) and contributions (F_i in %) to the spectral signal (with the total change of the CD or fluorescence signal taken as 100%) are presented on Fig. 1. The % contributions to the total signal, F_i, were calculated according to the formula:

$$F_i = 100\frac{f_{i+1} - f_i}{f_{n+2} - f_1}, \quad \text{where} \quad i = 1, \ldots\ldots, n+1. \qquad \text{[S5]}$$

Thermodynamic Activation Parameters. Using kinetic measurements at various temperatures, the activation energies E_i^a for each transition were calculated from Arrhenius plots (Fig. 3*B*) according to the Arrhenius equation:

$$\ln k_i = -\frac{E_i^a}{RT}, \qquad \text{[S6]}$$

where k_i are the rates presented in the Table S2, R is the gas constant, and T is the absolute temperature. Assuming that the transition from one intermediate to another occurs through a single transition state, the Eyring equation can be applied for the calculation of the activation enthalpy $\Delta H_i^{\#}$ and the activation entropy $\Delta S_i^{\#}$ associated with the transitions from one intermediate to another:

$$\ln\left(\frac{hk_i}{k_b T}\right) = -\frac{\Delta H_i^{\#}}{RT} + \frac{\Delta S_i^{\#}}{R}. \qquad \text{[S7]}$$

The activation Gibbs free energy, $\Delta G_i^{\#}$ is then

$$\Delta G_i^{\#} = \Delta H_i^{\#} - T\Delta S_i^{\#}, \qquad \text{[S8]}$$

where h is Planck's constant and k_b is Boltzmann's constant.

1. Reshetnyak YK, Andreev OA, Segala M, Markin V, Engelman DM (2008) Energetics of peptide (pHLIP) binding to and folding across a lipid bilayer membrane. *Proc Natl Acad Sci USA* 105:15340–15345.

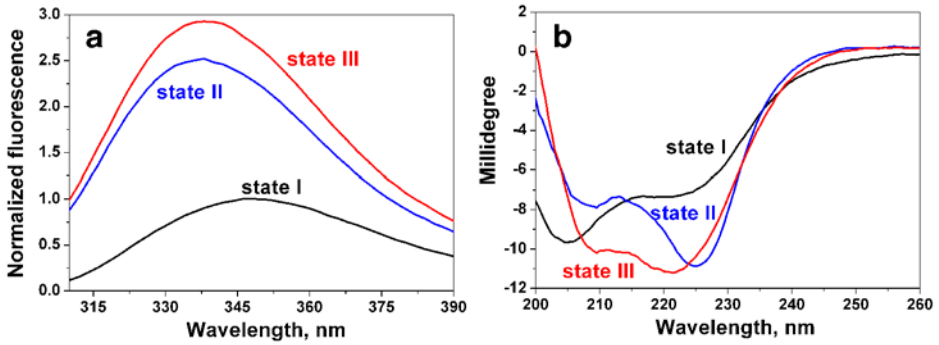

Fig. S1. The fluorescence (*A*) and CD (*B*) spectra of variant pHLIP with the Pro replaced by Ala in the middle of the transmembrane part. Spectra are presented at pH8.0 in the absence (*Black Lines*) and presence (*Blue Lines*) of vesicles and at pH4.0 in the presence of vesicles (*Red Line*).

Table S1. The transition rates, k_i, (fractional contributions, F_i) and goodness-of-fit (adjusted R-square, *adjR*^{2}, and root mean squared error, *RMSE*), were obtained by fitting the fluorescence kinetic curves measured at various temperatures presented in Fig. 3*A* and using Eq. S3

Temperature	k_1, s^{-1} (F_1, %)	k_2, s^{-1} (F_2, %)	k_3, s^{-1} (F_3, %)	k_{4X}, s^{-1} (F_4, %)	*adj* R^2/*RMSE*
7°C 11°C 18° C 25°C 37° C	> 40 (13.0) > 30 (18.0) > 30 (21.2) > 35 (23.1) > 35 (23.0)	0.48 (13.7) 0.52 (14.2) 0.69 (16.8) 0.89 (16.3) 1.83 (18.2)	0.050 (39.4) 0.053 (37.8) 0.071 (32.4) 0.106 (27.5) 0.266 (27.7)	0.0110 (33.9) 0.0131 (30.0) 0.0196 (29.6) 0.0242 (33.1) 0.0454 (31.1)	0.99998/4.08E-40.99998/ 4.05E-40.99997/4.86E-40.99996/5.27E-40.99963/ 1.46E-3

The rates k_2– k_4 have relative 95% confidence bounds of 1% or better. Due to an insufficient number of experimental points within first 50 ms, only a lower bound was estimated for the first rate (k_1).

Table S2. Activation thermodynamics parameters are presented for the transitions from one intermediate to another during the process of folding and insertion

	I_1 I_2 *	I_2 I_3	I_3 I_4	I_4 I_5
ΔE_a, kcal/mol$\Delta H^{\ddagger}$, kcal/mol$\Delta S^{\ddagger}$, cal/(K·mol)$\Delta G^{\ddagger}$, kcal/mol at 25 °C	-0.4 ± 0.8-1.0 ± 0.8-54.7 ± 2.915.4	7.1 ± 0.87.7 ± 0.8-34.8 ± 2.717.5	9.1 ± 1.29.7 ± 1.3-32.1 ± 4.318.7	7.4 ± 0.48.0 ± 0.4-40.8 ± 1.319.6

The activation energy, $E^a{}_i$, was calculated from the Arrhenius plots (Fig. 3*B*) according to the Arrhenius equation (Eq. **S6**). The activation enthalpy $\Delta H_i^{\#}$ and the activation entropy $\Delta S_i^{\#}$ were calculated according to the Eyring equation (Eq. **S7**). The activation Gibbs free energy, $\Delta G_i^{\#}$ at 25 °C was calculated according to the Eq. **S8**.

*The data presented for the first transition are not statistically significant because the correlation coefficient $R < 0.5$ and the p-level $p > 0.3$. All parameters calculated for other transitions are statistically significant, $R > 0.973$ and $p < 0.0053$.